molecular pharmaceutics

Communication

pubs.acs.org/molcularpharmaceutics

Efficacy of PolyMPC−DOX Prodrugs in 4T1 Tumor-Bearing Mice

Samantha McRae Page,[†,‡] Elizabeth Henchey,[‡,§] Xiangji Chen,[†] Sallie Schneider,*[,§] and Todd Emrick*[,†]

[†]Polymer Science & Engineering Department, University of Massachusetts, 120 Governors Drive, Amherst, Massachusetts 01003, United States

[§]Pioneer Valley Life Sciences Institute, 3601 Main Street, Springfield, Massachusetts 01199, United States

Supporting Information

ABSTRACT: We report the *in vivo* efficacy, in tumor-bearing mice, of cancer prodrugs consisting of poly(methacryloyloxyethyl phosphorylcholine) (polyMPC) conjugated to doxorubicin (DOX). Our synthesis of polyMPC−DOX conjugates established prodrugs with tunable drug loading, pH sensitive release kinetics, and a maximum tolerated dose in the range of 30−50 mg/kg (DOX equivalent) in healthy mice. Here we show prolonged circulation of polyMPC−DOX, with a measured *in vivo* half-life ($t_{1/2}$) 8 times greater than that of the free drug. We observed reduced drug uptake in healthy tissue, and 2−3 times enhanced drug accumulation in tumors for polyMPC−DOX prodrugs compared to free DOX, using BALB/c mice bearing 4T1 tumors. Prolonged survival and reduced tumor growth were observed in mice receiving the polyMPC−DOX prodrug treatment. Moreover, we evaluated immunogenicity of polyMPC−DOX prodrugs by examining complete blood count (CBC) and characteristic cytokine responses, demonstrating no apparent innate or adaptive immune system response.

KEYWORDS: *polymer−drug conjugate, polymer prodrug, poly(methacryloyloxyethyl phosphorylcholine), doxorubicin, drug delivery*

INTRODUCTION

Nanoscale therapeutics based on synthetic polymer scaffolds offers new routes to improved cancer drug delivery,[1−3] with water-soluble polymers aiding in drug solubility, increasing the therapeutic window through long circulation half-life ($t_{1/2}$), and increasing uptake into tumors by the enhanced permeability and retention (EPR) effect.[4] For polymer-based prodrugs, recent interest centers on triggered release of therapeutic moieties from the polymer scaffold,[5] for example by exploiting intratumoral or intracellular environmental triggers such as pH.[6−8] This approach is intended to reduce nonspecific, off-target toxicity often associated with systemic delivery.

We reported the preparation of poly(2-methacryloyloxyethyl phosphorylcholine)−doxorubicin (polyMPC−DOX) prodrugs, in which DOX was connected to the polymer backbone by hydrazone linkages, which are pH sensitive.[9] These prodrugs were prepared by copolymerization of MPC with methacrylates containing pendent acyl hydrazides and then incorporating DOX by hydrazone formation, to give tunable DOX loading that can reach or exceed 30 wt %. These polyMPC−DOX conjugates displayed pH sensitive release profiles, with half-life ($t_{1/2}$) values ranging from 2 to 40 h at pH 5.0, while only 2 to 20% of DOX was released in 48 h at pH 7.4. In cell culture, the half-maximal inhibitory concentration (IC_{50}) values for polyMPC−DOX ranged from 1.5 to 16 μM for human breast cancer (MCF-7 and MDA-MB-231) and colorectal (COLO 205) adenocarcinoma cell lines.[9] This initial synthesis and cell culture characterization suggested polyMPC−DOX conjugates as potentially efficacious for tumor reduction *in vivo*.

Here, we report *in vivo* pharmacokinetic, biodistribution, and treatment efficacy data for polyMPC−DOX using a 4T1 murine breast cancer model. The 4T1 mammary carcinoma was selected as an extremely aggressive breast cancer model that is highly tumorigenic and metastatic, and thus can be considered as a model for triple negative breast cancer.[10,11] Unlike many tumor models, 4T1 tumors can metastasize spontaneously from the primary tumor to multiple distant sites including the lungs, lymph nodes, liver, brain, and bone within weeks following injection.[10] We viewed the 4T1 model as a challenging tumor model to test polyMPC−DOX prodrugs, potentially enhancing the utility of DOX in late stage breast cancer. 4T1 cells can be introduced orthotopically by direct injection into the mammary gland, such that the primary tumor site is anatomically correct, and the syngeneic nature of the cells allows for use of immunocompetent animals, and thus examination of the effects of polyMPC−DOX conjugates on the immune system. The 4T1 breast cancer model has been used by others to study polymer prodrugs *in vivo*, including paclitaxel,[12,13] docetaxel,[12] cisplatin,[14,15] gemcitabine,[16] and doxorubicin,[17,18] with variable success with respect to slowing tumor growth and reducing off-target toxicity. Given the high level of water solubility and degree of drug loading achievable with polyMPC−DOX prodrugs, this study aimed to demonstrate their efficacy in 4T1 tumor-bearing mice.

MATERIALS AND METHODS

Methacryloyloxyethyl phosphorylcholine (MPC), ethyl bromoacetate, copper(I) bromide, 2,2′-bipyridine (bpy), ethyl

Received: January 5, 2014
Revised: April 2, 2014
Accepted: April 9, 2014
Published: April 21, 2014

2-bromoisobutyrate (EBiB), hydrazine monohydrate, acetic acid, magnesium sulfate, trifluoroacetic acid (TFA), acetonitrile (anhydrous), methanol (anhydrous), and dimethyl sulfoxide (anhydrous) were purchased from Aldrich. DOX was purchased from 21CEC. Spectra/Por 3 dialysis membrane (MWCO 1000) was purchased from Spectrum Laboratories, Inc. Sephadex (LH-20 and G-25) was purchased from GE Life Sciences. Hanks balanced salt solution used for *in vivo* studies was obtained from Life Technologies (Gibco).

Instrumentation. NMR spectra were recorded on a Bruker DPX300 spectrometer. UV/vis absorbance measurements were taken on a PerkinElmer Lambda 25 spectrometer. Molecular weights and polydispersity indices (PDIs) were estimated by gel permeation chromatography (GPC) in sodium nitrate (0.1 M with 0.02 wt % of NaN_3) aqueous solution against poly(ethylene oxide) standards, operating at 1.0 mL/min with three Waters Ultrahydrogel Linear columns (300 × 7.8 mm) equipped with RI and UV detectors. HPLC was performed on a Waters Alliance system equipped with UV and fluorescence detectors. A reverse phase C18 column (250 × 4.6 mm) eluting with 40% acetonitrile in water + 1% TFA at a flow rate of 1 mL/min was used to analyze biological samples obtained from the pharmacokinetic and biodistribution studies.

Synthesis of 2-Ethoxy-2-oxoethyl Methacrylate (EtOEMA). Sodium methacrylate (9.7 g, 90 mmol) and 10.02 g of ethyl bromoacetate (60 mmol) were added to 55 mL of dry acetonitrile. To this suspension was added 3.5 g of tetrabutylammonium bromide (TBAB). The reaction mixture was heated to reflux overnight. The salt was removed by filtration, and solvent was removed by evaporation under reduced pressure. The residue was redissolved in ethyl acetate and washed four times with water. The organic phase was dried over $MgSO_4$, and concentration under vacuum gave the desired monomer as a pale yellow oil (9.8 g, 95%). ^{1}H NMR ($CDCl_3$, 300 MHz): δ 6.21 (s, 1H), 5.64 (m, 1H), 4.66 (s, 2H), 4.22 (q, 2H), 1.97 (s, 3H), 1.27 (t, 3H) ppm. ^{13}C NMR ($CDCl_3$, 75 MHz): δ 167.9, 166.7, 135.4, 126.8, 61.4, 60.9, 18.2, 14.1 ppm.

General Procedure for ATRP Copolymerization To Prepare Polymer 4. EBiB (5.9 mg, 0.03 mmol), MPC, and EtOEMA were combined in a 10 mL two-neck round-bottom flask, and three cycles of vacuum−nitrogen were employed. DMSO and MeOH (previously degassed with $N_{2(g)}$) were injected with a degassed syringe. The mixture was purged with $N_{2(g)}$ for 20 min. Cu(I)Br (8.6 mg, 0.06 mmol) and bipyridine (18.7 mg, 0.12 mmol) were added quickly as solids under nitrogen atmosphere. The mixture was then purged with nitrogen gas for an additional 20 min and then left under nitrogen atmosphere. The mixture was stirred at room temperature, and the polymerization conversion was monitored by ^{1}H NMR spectroscopy. The polymerization was terminated by exposure to air. The crude product was purified by column chromatography on silica gel, eluting with methanol to give the poly(MPC-EtOEMA) **3** random copolymer as a white solid. The monomer ratio in the copolymer was characterized by ^{1}H NMR spectroscopy, integrating signals at 3.58 ppm ($-CH_2-$N in MPC) and at 1.27 ppm (($-CH_3$) in EtOEMA). Poly(MPC-EtOEMA) was dissolved in methanol at a concentration of 100−200 mg/mL. Hydrazine monohydrate was added to the polymer solution to a final concentration of 25%. The reaction mixture was stirred at room temperature, with monitoring by ^{1}H NMR spectroscopy. Upon completion, the reaction mixture was diluted with water and purified by dialysis against water using a MWCO 1000 membrane for 2 days and passing through a 0.45 μm membrane. Copolymer **4** was obtained as a white powder after lyophilization. The typical yield was over 80%, and the loading of the hydrazine group was calculated by integration of signals at 3.58 ppm ($-CH_2-$N in MPC) and 4.64 ppm ($-CH_2-CONHNH_2$) in the ^{1}H NMR spectrum. ^{1}H NMR (MeOD, 300 MHz): δ = 0.9−1.2 (br, 3H), 1.8−2.3 (br, 2H), 3.3 (s, 9H), 3.75 (br, 2H), 4.16 (br, 2H), 4.3 (br, 2H), 4.38 (br, 2H), 4.64 (br, 2H). ^{13}C NMR (MeOD, 100 MHz): δ = 16.8, 18.5, 44.7, 45.0, 53.4, 59.3, 62.2, 62.9, 64.8, 66.1, 167.1, 176.9, 178.1. GPC (0.1 M $NaNO_3$ + 0.02 wt % NaN_3, PEO standards): M_n, 25,000; PDI 1.4. Hydrazine loading of copolymer **4** by ^{1}H NMR spectroscopy: 19 mol %.

Synthesis of Polymer−DOX Prodrug 5. MPC copolymer **4** (200 mg, 0.165 mmol of $-NHNH_2$) and DOX (58 mg, 0.1 mmol) were dissolved in anhydrous methanol (5 mL). To this solution were added 60 μL of acetic acid and 200 mg of anhydrous magnesium sulfate. The reaction mixture was stirred in the dark at room temperature for 2 days. The resulting conjugate was purified by passage over a Sephadex LH-20 column eluting with methanol. Fractions containing polymer−DOX conjugate were concentrated by rotary evaporation, redissolved in water, and further purified by Sephadex G-25 column eluting with pure water. PolyMPC−DOX conjugate **5** was obtained as a dark red powder after lyophilization (230 mg, 88%).

Determination of DOX Loading. DOX·HCl was dissolved in pure water at 0.01 mg/mL, and polyMPC−DOX conjugate **5** was dissolved in pure water at a concentration of 0.1 mg/mL. The DOX loading of the conjugate was calculated on the basis of UV/vis absorbance at 490 nm, using the molar absorptivity of DOX·HCl at 490 nm.

Pharmacokinetics and Biodistribution in Animals. All experiments were performed in accordance with protocols approved by the Baystate Institutional Animal Care and Use Committee. Four week old BALB/c female mice were injected subcutaneously in the right flank with 5 × 10^6 4T1 murine breast cancer cells suspended in 100 μL of Hanks balanced salt solution (HBSS). Once tumors reached a size of 100−300 mm^3 (calculated by length × width^2 × π/6), mice were injected through the lateral tail vein with 100 μL of HBSS, free doxorubicin (6 mg/kg), or polyMPC−DOX (6 mg/kg, DOX equivalent) (n = 8/treatment). Blood samples (30−50 μL) were taken from the submandibular vein prior to injection, and then 30 min, 2 h, 6 h, 12 h, 1 day, 2 days, 3 days, and 5 days postinjection. Blood samples were clotted on ice and centrifuged at 1500g for 15 min at 4 °C. Serum was collected and stored at −80 °C until HPLC analysis to determine doxorubicin concentration. On day 3 and day 5 postinjection, mice were euthanized from each treatment group. Blood was collected by cardiac puncture (800 μL), and a complete blood count (CBC) was performed on 500 μL using the VetScan HM5. The remaining samples were allowed to clot on ice, and centrifuged at 1500g for 15 min at 4 °C. Serum was collected and stored at −80 °C for ELISA of cytokine response. Tumor, heart, liver, lung, kidney, and spleen samples were collected, weighed, and frozen in liquid nitrogen. Livers and spleens were divided, and half of each tissue was additionally fixed in 10% buffered formalin overnight at 4 °C, transferred to 70% EtOH at 4 °C, and paraffin embedded for histological analysis. Frozen tissues were homogenized at maximum speed in acidified isopropanol (90% isopropanol containing 0.6 mL of concentrated HCl). Samples were then centrifuged at 1500g for 15 min at 4 °C, and the upper aqueous phase was collected and

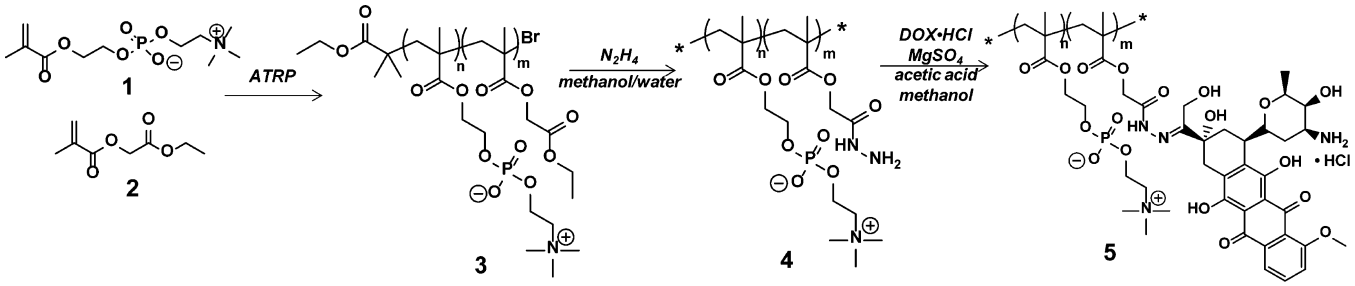

Figure 1. Synthesis of poly(MPC-*co*-EtOEMA) (**3**), followed by acylhydrazine formation (**4**) and conjugation of DOX·HCl to give polyMPC−DOX prodrug (**5**).

stored at −80 °C until HPLC analysis of doxorubicin concentration.

***In Vivo* Antitumor Efficacy.** Four week old BALB/c female mice were injected into lower right mammary fat pad with 5×10^6 4T1 murine breast cancer cells suspended in 100 μL of Hanks balanced salt solution (HBSS). Once tumors reached a size of 42−132 mm^3 (calculated by length × width^2 × π/6), mice were injected through the lateral tail vein with free doxorubicin (3 mg/kg), polyMPC−DOX (15 mg/kg DOX equivalent), or HBSS (control) (n = 15/treatment). A second injection of the same concentration was given on day 7, and mice treated with polyMPC−DOX received a third dose on day 17. Animals were monitored for signs of distress, and body weights and tumor measurements were collected every 2 days. Upon completion, tumor, heart, liver, lung, kidney, and spleen samples were collected, weighed, and fixed in 10% buffered formalin overnight at 4 °C, transferred to 70% EtOH at 4 °C, and paraffin embedded for histological analysis.

RESULTS AND DISCUSSION

PolyMPC−DOX prodrugs were prepared by copolymerization of MPC with 2-ethoxy-2-oxoethyl methacrylate (EtOEMA) by atom transfer radical polymerization (ATRP) using copper bromide and bipyridine as the catalyst and ligand, respectively.[9] The ethyl esters of copolymer **3** are converted to acylhydrazines by substitution with hydrazine to give polyMPC-hydrazine, shown as polymer **4** in Figure 1. Polymer **4** was characterized by aqueous gel permeation chromatography (GPC) against linear PEO standards, and by ^{1}H NMR spectroscopy to determine the mole percent of hydrazine monomer units within the polymer. Under these conditions, hydrazine substitution was preferred at the ketone of the ethyl ester, as confirmed by NMR spectroscopy noting loss of the ethyl ester methyl group at 1.25 ppm, and retention of the methylene ($-CH_2-CONHNH_2$) at 4.64 ppm. The mole percent incorporation of comonomer remained constant through the transition from copolymer **3** to polyMPC-hydrazine **4**. Polymer **4** was conjugated to DOX by hydrazone formation in methanol, in the presence of magnesium sulfate and acetic acid, to give polyMPC−DOX prodrug **5**. PolyMPC−DOX **5** was purified by preparative size exclusion chromatography and lyophilized to give a bright red powder, which proved stable for months when stored as a dry solid at −20 °C. For the efficacy study described here, we used polyMPC−DOX with an estimated molecular weight of 25 000 g/mol, and DOX loading of 22 wt %.

We previously reported maximum tolerated dose (MTD) data for polyMPC−DOX in athymic Nu/j mice, where polyMPC−DOX was found to be well-tolerated at 30 mg/kg over the course of 30 days; mice which received doses of 50 mg/kg showed only a 10% weight loss at 22 days.[9] These values represent an increase over the MTD of free DOX (~6 mg/kg),[19] and are comparable to the liposomal formulation DOXIL (20−30 mg/kg)[20] and a PEGylated polyester dendritic DOX example (20−40 mg/kg).[20] To further extend our *in vivo* prodrug characterization, the pharmacokinetics of polyMPC−DOX were evaluated in BALB/c mice. Animals were sorted into three groups of eight, with a control group (HBSS), a free DOX group, and a polyMPC−DOX group (6 mg/kg DOX equivalent doses), introducing drugs by a single tail vein injection of 100 μL total volume. Blood serum levels of DOX were monitored over time, analyzing for the presence of drug by HPLC equipped with a fluorescence detector. As shown in Figure 2, *in vivo* free DOX concentration decreased rapidly,

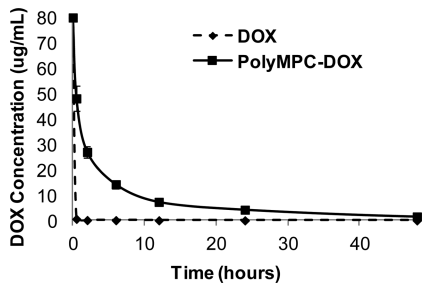

Figure 2. Pharmacokinetic analysis of polyMPC−DOX in BALB/c mice. Polymer conjugation extends the circulation half-life from 15 min to 2 h and increases the AUC from 22 μg·h/mL to 408 μg·h/mL. Error bars represent ± standard deviation.

Table 1. Tumor to Normal Tissue Distribution Ratios for PolyMPC−DOX and DOX

	day	liver	spleen	lung	heart	kidney
polyMPC−DOX	3	0.52	1.50	1.86	4.00	0.90
	5	0.66	2.40	2.45	5.94	0.94
free DOX	3	0.83	0.35	0.45	2.01	0.39
	5	0.63	0.21	0.33	1.43	0.49

with a $t_{1/2}$ of 15 min, clearing to near-undetectable levels within 1 h. This is consistent with reported values for DOX.[17,19] PolyMPC−DOX displayed a significantly longer circulation half-life of 2 h. Accordingly, the area under the curve (AUC) was dramatically higher for the polyMPC−DOX prodrug (408 μg·h/mL) compared to free DOX (22 μg·h/mL).

The biodistribution of DOX was determined for both the free drug and polyMPC−DOX, 3 and 5 days postinjection from the 6 mg/kg DOX equivalent doses administered to the tumor-bearing mice used in the PK study (Figure 3). The tumor

dx.doi.org/10.1021/mp500009r | *Mol. Pharmaceutics* 2014, 11, 1715−1720

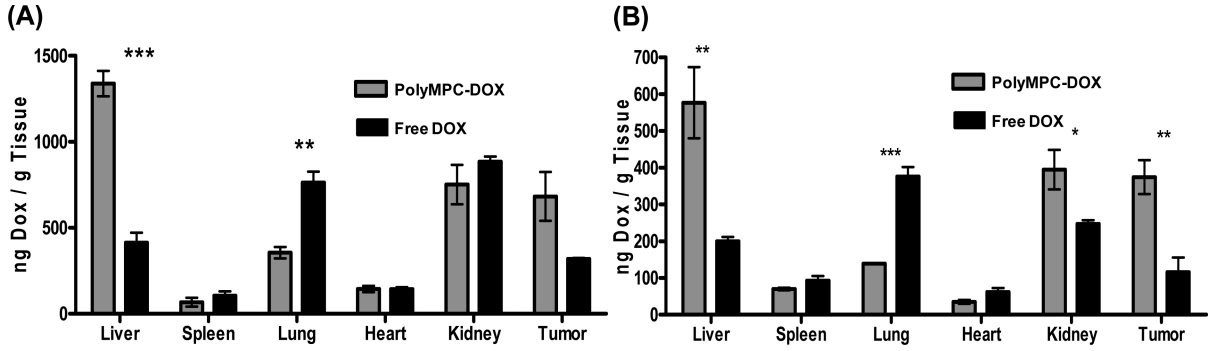

Figure 3. Biodistribution analysis of polyMPC−DOX and free DOX after (A) 3 days and (B) 5 days, expressed as ng of DOX/g of tissue. The significance was determined using a two-tailed Student *t* test [$*p$ = 0.05 to 0.01; $**p$ = 0.01 to 0.001; $***p < 0.001$]. Error bars represent ± the standard error of the mean (SEM).

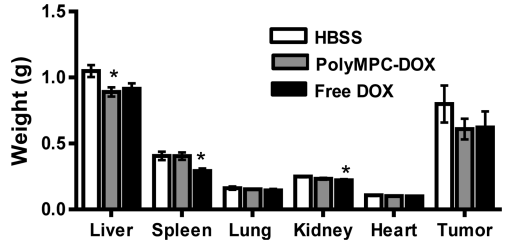

Figure 4. Weights (g) of tissues collected at conclusion of the study (5 days postinjection): liver, spleen, lung, kidneys, heart, and tumor. Error bars represent ± SEM ($*p$ = 0.5−0.1).

uptake of DOX for polyMPC−DOX was 700 ng/g of tissue 3 days after injection, and 390 ng/g 5 days after injection. This represents a 2-fold increase over free DOX at day 3 (350 ng/g) and a 3-fold increase over free DOX at day 5 (130 ng/g). Moreover, polyMPC−DOX conjugates displayed reduced accumulation in off-target organs, including the spleen and especially the lungs, relative to free DOX. Significantly higher drug accumulation was noted in the liver for the polyMPC−DOX group compared to the free DOX group, which we attribute to the prolonged circulation times and the delayed clearance noted for the polymer prodrug. While DOX is known to be metabolized primarily by the liver, the liposomal formulation DOXIL was found to have impaired hepatic metabolism, suspected to be excluded from uptake based on the liposome size.[21] Similarly, the increased size of polyMPC−DOX prodrugs relative to free DOX may hamper hepatic uptake, resulting in delayed accumulations. Low drug accumulation found in the heart for the polyMPC−DOX group is potentially advantageous for reducing cardiotoxicity effects, a common dose-limiting side effect associated with DOX administration.[22] The tumor to normal tissue distribution ratios are given in Table 1, highlighting the preferential DOX uptake in tumor tissue relative to healthy tissue. The benefits of passive tumor targeting of polymer prodrugs has been noted before,[4,17] and the data presented here suggests that the polyMPC−DOX has similar benefits *in vivo*.

At the conclusion of the PK and biodistribution study, the spleen, liver, kidney, heart, lungs, and tumors were removed

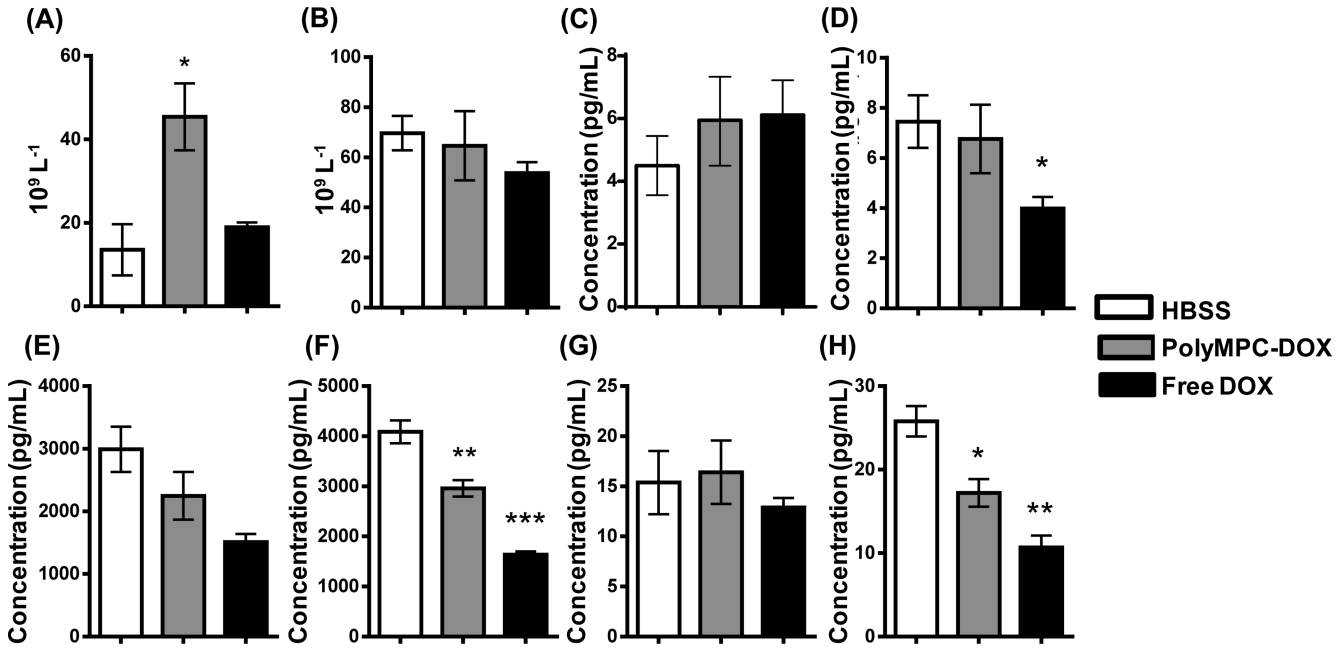

Figure 5. Analysis of immune response across all treatment groups using complete blood count (CBC) and ELISA cytokine measurements 3 and 5 days after injection: (A) white blood cell count (WBC) (day 3); (B) WBC (day 5); (C) interferon-γ (IFN-γ) (day 3); (D) IFN-γ (day 5); (E) interleukin-12 (IL-12) (day 3); (F) IL-12 (day 5); (G) interleukin-10 (IL-10) (day 3); (H) IL-10 (day 5). Error bars represent ±SEM.

dx.doi.org/10.1021/mp500009r | *Mol. Pharmaceutics* 2014, 11, 1715−1720

from the animals and weighed, with livers and spleens fixed and paraffin-embedded for histological analysis. As shown in Figure 4, only small differences among the groups were noted with respect to tissue weights. Histological analysis of tissue sections stained with hematoxylin and eosin (H&E) suggested no significant off-target toxicity at these high levels of DOX, consistent with the use of polyMPC as the carrier. Despite the noted increase in drug accumulation in the liver, H&E analysis revealed no sign of adverse effects or off-target toxicity in the liver (Figure S1 in the Supporting Information).

While our data, and other literature reports on polyMPC, point to the safety of its use *in vivo*, we are not aware of prior reports that examine potential *in vivo* immunogenicity arising from its presence in the bloodstream. Thus, in conjunction with these *in vivo* efficacy studies, we sought to gauge whether there were innate or adaptive immune system responses to polyMPC, accomplished through a complete blood count (CBC), and measurement of cytokine responses by an enzyme-linked immunosorbent assay (ELISA) (Figure 5). Analysis of serum cytokine and white blood cell (WBC) levels indicated an initial increase in total WBC count on day 3 with polyMPC−DOX (Figure 5A), with no differences noted on day 5 (Figure 5B). The initial increase in white blood cell count, suggestive of a foreign antigen response, was rectified by day 5. Red blood cell (RBC) counts indicated no differences across the treatment groups. Furthermore, we observed no significant differences between polyMPC−DOX and HBSS in Th1 versus Th2 cytokines by ELISA at day 3, with only a slight decrease in IL12 and IL10 noted at day 5. However, this cannot be attributed to the polyMPC carrier, since this decrease is much more pronounced in the case of animals treated with free DOX (Figures 5C−5H). These results suggest that polyMPC-bound DOX does not elicit significant adverse immunogenic effects that would produce undesired anemia or inflammatory response in animals.

4T1 tumor-bearing mice were used to evaluate the therapeutic performance of polyMPC−DOX conjugates for the treatment of breast cancer. Tumors were established by orthotopic injection of murine 4T1 cells (5×10^6 4T1 cells in Hanks balanced salt solution, HBSS) into the mammary fat pad of the mice (~17.5 g, 4 weeks old). The mice were randomized into three groups of 15; at a tumor volume in the range of 42−132 mm^3, mice were administered either HBSS, free DOX (3 mg/kg, ~1/2 MTD), or polyMPC−DOX (15 mg/kg DOX equivalent, ~1/2 MTD) by tail vein injection. Subsequent doses were administered on days 7 and 17 (polyMPC−DOX group only). Mice were examined and weighed every 2−4 days, and tumor volume was determined by caliper measurements (calculated by $0.52 \times L \times W^2$) over a period of 29 days. Mice were removed from the study when the tumor volume reached 1500 mm^3, if weight loss exceeded 20%, or if the animal showed signs of stress, such as a scruffy appearance or abnormal behavior. A summary of tumor efficacy results is presented in Figure 6. Figure 6A shows that survival increased substantially for mice receiving polyMPC−DOX compared to both the untreated and free DOX treated mice. Notably, mice receiving the free DOX treatment showed no improvement, essentially mirroring results for the HBSS group; all these mice were removed from the study by day 18. In contrast, 80% of the mice receiving the polyMPC−DOX treatment remained in the study at day 18, with overall survival in the polyMPC−DOX group extended almost 2-fold (29 days) compared to the other treatment groups. Figure 6B shows that tumor growth was greatly suppressed in the mice receiving polyMPC−DOX,

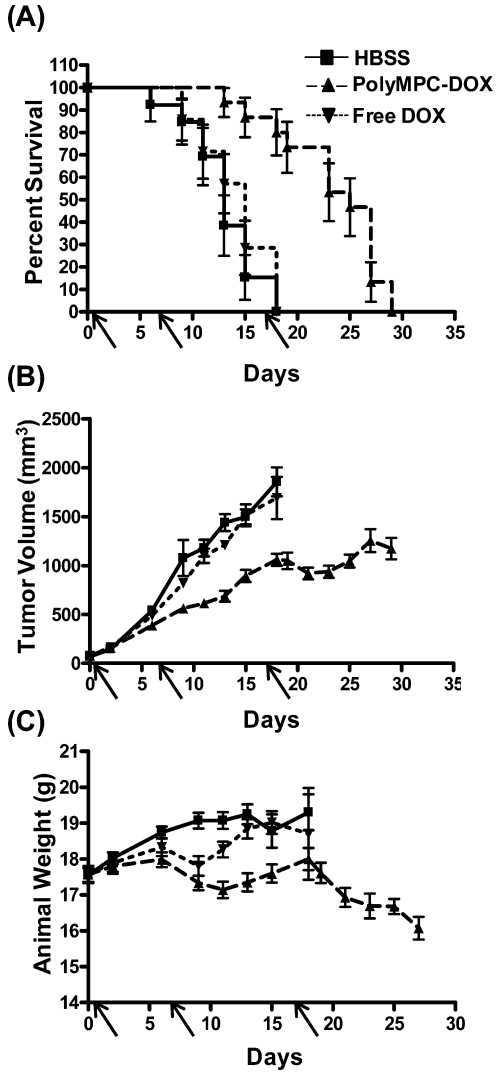

Figure 6. Summary of efficacy data in 4T1 mouse model: (A) survival curve for mice treated with HBSS (squares, solid line), polyMPC−DOX (triangles, dashed line), and free DOX (inverted triangle, dotted line); (B) tumor growth over time for mice treated with HBSS (squares, solid line), polyMPC−DOX (triangles, dashed line), and free DOX (inverted triangle, dotted line); (C) mouse weight for mice treated with HBSS (squares, solid line), polyMPC−DOX (triangles, dashed line), and free DOX (inverted triangle, dotted line) Arrows indicate days on which treatments were administered: 0, 7, and 17 (polyMPC−DOX only). Error bars represent ±SEM.

whereas the mice receiving free DOX showed no difference relative to the untreated mice. Untreated and free DOX treated mice surviving to day 18 displayed tumors with average volumes ranging from 1600 to 1850 mm^3, requiring their removal from the study. PolyMPC−DOX treated mice at day 18 had average tumor volumes of 1050 mm^3, and at the day 29 end point, average tumor volume was 1170 mm^3. The weights of the mice overall remained largely unchanged over the course of the study, as shown in Figure 6C. However, following the third dose of polyMPC−DOX, animal weights did not return to the normal range, necessitating their removal from the study. At the conclusion of the study, tissue samples (liver, spleen, heart, kidney) were collected and analyzed to compare to the results obtained from the PK/biodistribution study, with the mice from the efficacy study displaying comparable tissue weights among the treatment groups, with the exception of the lungs (Figure S2

dx.doi.org/10.1021/mp500009r | *Mol. Pharmaceutics* 2014, 11, 1715−1720

in the Supporting Information). The significant weight increase in the lungs of the polyMPC−DOX group is attributed to the numerous metastases in the lungs, likely due to the prolonged survival of the mice in this group (two times that of the free DOX and HBSS mice). H&E analysis indicated no apparent off-target toxicity in the liver even at the higher doses of polyMPC−DOX used in the efficacy study, despite the previously noted accumulation (Figure S3 in the Supporting Information). We note that the mice receiving polyMPC−DOX treatment were dosed below the previously determined MTD for these conjugates, so that the cumulative dose received did not exceed the MTD. Since the PK data reveals that polyMPC−DOX is nearly cleared within 48 h, future animal studies will examine a more frequent dosing regimen, aiming toward complete tumor regression. Nonetheless, this experiment confirms the efficacy of polyMPC−DOX prodrugs, even when presented with aggressive, highly metastatic 4T1 cancer in live animals.

■ CONCLUSIONS

The present study demonstrates the ability of polyMPC−DOX to prolong circulation half-life of DOX from 15 min to 2 h, with more favorable drug accumulation in the tumor as opposed to healthy tissue, and no significant innate or adaptive immunogenic response. Moreover, we demonstrate the efficacy of polyMPC−DOX in 4T1 tumor-bearing mice, increasing the overall survival 2-fold, and significantly reducing tumor growth in mice. The aggressive 4T1 mouse model reveals the potential for polyMPC−DOX in the treatment of triple negative breast cancer, and ongoing studies include evaluating the *in vivo* efficacy against a human breast cancer cell line.

■ ASSOCIATED CONTENT

Ⓢ Supporting Information

H&E staining of livers and tissue weights at the conclusion of the efficacy study. This material is available free of charge via the Internet at http://pubs.acs.org.

■ AUTHOR INFORMATION

Corresponding Authors

*E-mail: sallie.schneider@baystatehealth.org.

*E-mail: tsemrick@mail.pse.umass.edu.

Author Contributions

‡These authors contributed equally to this work.

Notes

The authors declare no competing financial interest.

■ ACKNOWLEDGMENTS

The authors acknowledge the National Institutes of Health for support under Award Number R21 CA167674 as well as an award from the Center for Excellence in Apoptosis Research (Massachusetts Technology Collaborative). We also acknowledge facilities support from the NSF Materials Research Science and Engineering Center (MRSEC) on Polymers at UMass (NSF-DMR-0820506). We thank Lotfi Bassa for assistance with the Mesoscale Discovery analysis of the serum cytokine levels, and Josephine Wyman and Brooke Bentley for their assistance with sectioning and staining tissues.

■ REFERENCES

(1) Davis, M. E.; Chen, Z.; Shin, D. M. Nanoparticle therapeutics: an emerging treatment modality for cancer. *Nat. Rev. Drug Discovery* **2008**, *7*, 771−782.

(2) Vicent, M. J.; Duncan, R. Polymer conjugates: nanosized medicines for treating cancer. *Trends Biotechnol.* **2006**, *24*, 39−47.

(3) Haag, R.; Kratz, F. Polymer therapeutics: Concepts and applications. *Angew. Chem., Int. Ed.* **2006**, *45*, 1198−1215.

(4) Maeda, H.; Wu, J.; Sawa, T.; Matsumura, Y.; Hori, K. Tumor vasculature permeability and the EPR effect in macromolecular therapeutics: a review. *J. Controlled Release* **2000**, *65*, 271−284.

(5) Oh, K. T.; Yin, H.; Lee, E. S.; Bae, Y. H. Polymeric nanovehicles for anticancer drugs with triggering release mechanisms. *J. Mater. Chem.* **2007**, *17*, 3987−4001.

(6) Tannock, I. F.; Rotin, D. Acid pH in tumors and its potential for therapeutic exploitation. *Cancer Res.* **1989**, *49*, 4373−4384.

(7) Engin, K.; Leeper, D. B.; Cater, J. R.; Thistlethwaite, A. J.; Tupchong, L.; McFarlane, J. D. Extracellular pH distribution in human tumors. *Int. J. Hyperthermia* **1995**, *11*, 211−216.

(8) Mellman, I.; Fuchs, R.; Helenius, A. Acidification of the endocytic and exocytic pathways. *Annu. Rev. Biochem.* **1986**, *55*, 663−700.

(9) Chen, X.; Parelkar, S. S.; Henchey, E.; Schneider, S.; Emrick, T. PolyMPC-Doxorubicin Prodrugs. *Bioconjugate Chem.* **2012**, *23*, 1753−1763.

(10) Pulaski, B. A.; Ostrand-Rosenberg, S. Mouse 4T1 Breast Tumor Model. *Curr. Protoc. Immunol.* **2001**, *39*, 20.2.1−20.2.16.

(11) Tao, K.; Fang, M.; Alroy, J.; Sahagian, G. G. Imagable 4T1 model for the study of late stage breast cancer. *BMC Cancer* **2008**, *8*, 228−246.

(12) Etrych, T.; Sirova, M.; Starovoytova, L.; Rihova, B.; Ulbrich, K. HPMA Copolymer Conjugates of Paclitaxel and Docetaxel with pH-Controlled Drug Release. *Mol. Pharmaceutics* **2010**, *7*, 1015−1026.

(13) Liu, Z.; Chen, K.; Davis, C.; Sherlock, S.; Cao, Q.; Chen, X.; Dai, H. Drug delivery with carbon nanotubes for in vivo cancer treatment. *Cancer Res.* **2008**, *68*, 6652−6660.

(14) Paraskar, A.; Soni, S.; Basu, S.; Amarasiriwardena, C. J.; Lupoli, N.; Srivats, S.; Roy, R. S.; Sengupta, S. Rationally engineered polymeric cisplatin nanoparticles for improved antitumor efficacy. *Nanotechnology* **2011**, *22*, 265101.

(15) Paraskar, A. S.; Soni, S.; Chin, K. T.; Chaudhuri, P.; Muto, K. W.; Berkowitz, J.; Handlogten, M. W.; Alves, N. J.; Bilgicer, B.; Dinulescu, D. M.; Mashelkar, R. A.; Sengupta, S. Harnessing structure-activity relationship to engineer a cisplatin nanoparticle for enhanced antitumor efficacy. *Proc. Natl. Acad. Sci. U.S.A.* **2010**, *107*, 12435−12440.

(16) Kiew, L. V.; Cheong, S. K.; Ramli, E.; Sidik, K.; Lim, T. M.; Chung, L. Y. Efficacy of Poly-L-Glutamic Acid-Gemcitabine Conjugate in Tumor-Bearing Mice. *Drug Dev. Res.* **2012**, *73*, 120−129.

(17) Zhou, L.; Cheng, R.; Tao, H.; Ma, S.; Guo, W.; Meng, F.; Liu, H.; Liu, Z.; Zhong, Z. Endosomal pH-Activatable Poly(ethylene oxide)-graft-Doxorubicin Prodrugs: Synthesis Drug Release, and Biodistribution in Tumor-Bearing Mice. *Biomacromolecules* **2011**, *12*, 1460−1467.

(18) Gao, Z.-G.; Tian, L.; Park, I.-S.; Bae, Y. H. Prevention of metastasis in 4T1 murine breast cancer model by doxorubicin carried by folate conjugated pH sensitive polymeric micelles. *J. Controlled Release* **2011**, *152*, 84−89.

(19) Kratz, F.; Azab, S.; Zeisig, R.; Fichtner, I.; Warnecke, A. Evaluation of combination therapy schedules of doxorubicin and an acid-sensitive albumin-binding prodrug of doxorubicin in the MIA PaCa-2 pancreatic xenograft model. *Int. J. Pharm.* **2013**, *441*, 499−506.

(20) Lee, C. C.; Gillies, E. R.; Fox, M. E.; Guillaudeu, S. J.; Frechet, J. M. J.; Dy, E. E.; Szoka, F. C. A single dose of doxorubicin-functionalized bow-tie dendrimer cures mice bearing C-26 colon carcinomas. *Proc. Natl. Acad. Sci. U.S.A.* **2006**, *103*, 16649−16654.

(21) Hilmer, S. N.; Cogger, V. C.; Muller, M.; Le Couteur, D. G. The hepatic pharmacokinetics of doxorubicin and liposomal doxorubicin. *Drug Metab. Dispos.* **2004**, *32*, 794−799.

(22) Safra, T.; Jeffers, S.; Tsao-Wei, D. D.; Groshen, S.; Lyass, O.; Henderson, R.; Berry, G.; Gabizon, A. Pegylated liposomal doxorubicin (doxil): Reduced clinical cardiotoxicity in patients reaching or exceeding cumulative doses of 500 mg/m^2. *Ann. Oncol.* **2000**, *11*, 1029−1033.